

TEMPERATURE DEPENDENCE OF THE STRUCTURAL AND OPTICAL PROPERTIES OF THE AMORPHOUS-TO-CRYSTALLINE TRANSITION IN AgSbSe₂ THIN FILMS

M. HAMAM, Y. A. EL-GENDY, M. S. SELIM^A, N. H. TELEB^A, A.M. SALEM^A

Faculty of Science, Helwan University, Cairo, Egypt

^aElectron Microscope and Thin films Department, Physics division, National Research Centre, Cairo, Egypt

Nearly stoichiometric thin films of the ternary AgSbSe₂ compound have been deposited at room temperature by conventional thermal evaporation of the presynthesized material onto glass substrate. The X-ray and electron diffraction studies revealed that the as-deposited films are amorphous in nature, while an amorphous-to-crystalline phase transition could be obtained by thermal annealing at 373 K. The elemental chemical composition of as-deposited films was confirmed using the energy dispersive X-ray analysis. The transmission spectra of the as-deposited and annealed films were recorded at normal light incidence in the wavelength range 600-2500 nm. The refractive index and optical band gap have been calculated for the investigated films. The dispersion parameters, (E_o , E_d) static refractive index $n_s(0)$, static dielectric constant, ϵ_s and the carrier concentration to the effective mass ratio, N/m^* have been calculated. An analysis of the optical absorption spectra revealed an direct optical transition characterizing the as-deposited films and those annealed at 343 and 374 K while; direct and indirect optical transitions characterized the films annealed at 398 K

(Received August 3, 2009; accepted September 15, 2009)

Keywords: AgSbSe₂, Thin films, XRD, Electron diffraction, amorphous-crystalline transition

1. Introduction

Due to extensive applications in solid-state devices and future prospects, chalcogenide glasses have received much attention in recent years. A good device is one that is of low cost, fast, accurate and easy to use. Amorphous selenium has been emerged as promising material because of its potential technological importance. It is widely preferred in the fabrication of electrophotographic devices and, more recently, switching and memory devices [1, 2] have found selenium-based materials to offer attractive advantages. The use of chalcogenide films for reversible optical recording by the amorphous-to-crystalline phase change has recently been reported [3].

Silver-containing chalcogenide glasses are considerable interest for applications in optical recording and as solid electrolytes. Therefore, the knowledge of optical, electrical, and structural properties of Ag-chalcogenide amorphous materials is of essential importance. The AgSbTe₂ [4], AgSbS₂ [5], and AgInSbSe₂ [6] systems have been previously studied, however, very little work concerning the optical and electrical properties of AgSbSe₂ have been presented [7-9]. In the present work, a systematic study of the structure and optical properties of thermally evaporated AgSbSe₂ thin films annealed at different temperatures has been studied. The effect of thermal annealing on the refractive index, high frequency dielectric constant (ϵ_∞), and carrier concentration to the effective mass ratio (N/m^*) were presented.

2. Experimental details

Polycrystalline ingot of the ternary AgSbSe_2 compound was prepared by the direct fusion of a mixture of the constituent elements in stoichiometric ratio, and purity 99.999%, in vacuum-sealed silica tube. Thin films were deposited by conventional thermal evaporation of the presynthesized material onto precleaned glass substrates held at room temperature, in $\sim 1.5 \times 10^{-3}$ Pa vacuum using a high vacuum coating unit (Type Edwards 306 A). The structural characteristics of the prepared ingot material as well as the as-deposited and annealed AgSbSe_2 films were examined by means of an X-ray diffractometer (Type Philips X'pert) with Ni-filtered CuK_α radiation operating at 35 kV and 100 mA. The chemical composition of the as-deposited films was identified using energy dispersive X-ray unit interfaced with a scanning electron microscope (Type JEOL-JSGM-T200). The microstructure of the as-deposited and annealed films was also examined using Transmission electron microscope (Type JEOL-JSGM-T1230). A double beam spectrophotometer, with automatic computer data acquisition (Type Jasco, V-570, Rer11-00, and UV-VIS-NIR), photometric accuracy of ± 0.002 – 0.004 absorbance and $\pm 0.3\%$ transmittance, was employed at normal light incidence to record the optical transmission and reflection spectra of the as-deposited and annealed films over the wavelength range 600–2500 nm. The thickness of the deposited films was from the interference fringes [10].

3. Results and discussion

3.1 Structural characterization

The X-ray diffractograms of the prepared AgSbSe_2 bulk material as well as the films annealed at different annealing temperatures, T_a are shown in Fig. 1a, b. Comparing the reflection planes of Fig.1-a with the standard XRD data (JCPDS cards no 12-0379), indicates that all the reflection planes can be indexed to the cubic phase of the ternary compound AgSbSe_2 with a cell parameter $a = 0.578$ nm. No reflections corresponding to any of the free elements or binary alloys were observed.

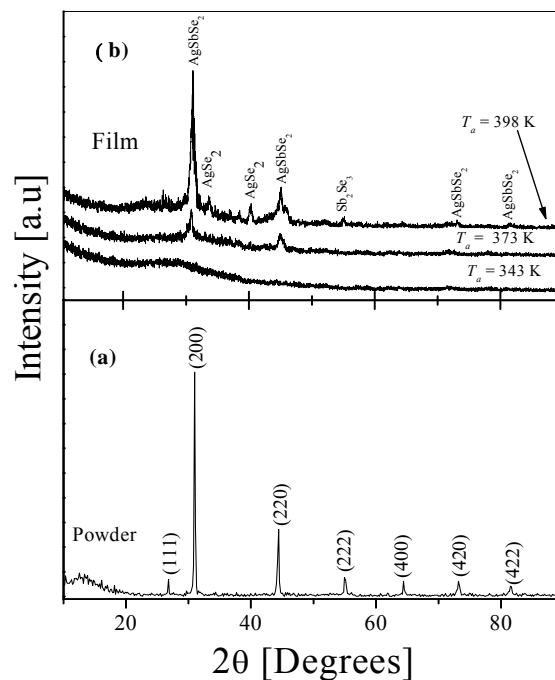


Fig.1 X-ray diffraction pattern of (a) the prepared AgSbSe_2 powder and (b) annealed films (of thickness 780 nm).

The XRD analysis, carried out on the as-deposited films (not given) and those annealed for 1 h in an Ar atmosphere at annealing temperatures $T_a < 343$ K are amorphous in nature, while those annealed at $T_a \geq 373$ K are crystalline. Analysis the XRD diffraction pattern of the films annealed at $T_a \geq 373$ K indicates that the film contains two peaks at $2\theta = 30.97^\circ$ and 44.39° , respectively, corresponding to reflections from (200), (220) planes of AgSbSe₂ single cubic phase. However, the XRD pattern for the film annealed at 398 K shows small diffraction peaks at $2\theta = 33.52^\circ$, 40.41° and 55.05° , respectively, corresponding to reflection from the (112), (122), and (514) planes, which belongs to the binary Ag₂Se, Sb₂Se₃ phases, beside AgSbSe₂ as a major phase.

Transmission electron micrographs of as-deposited AgSbSe₂ films, and those annealed at $T_a \leq 343$ K showed no discernible structure (See Fig.2). The corresponding diffraction patterns exhibited diffuse rings confirming the amorphous nature of the films as revealed by X-ray diffraction. On the films being annealed at $T_a \geq 373$ K, a distinct structure was observed in the transmission mode. The corresponding selected area diffraction shows crystallization of the films, as identified previously via X-ray diffraction analysis.

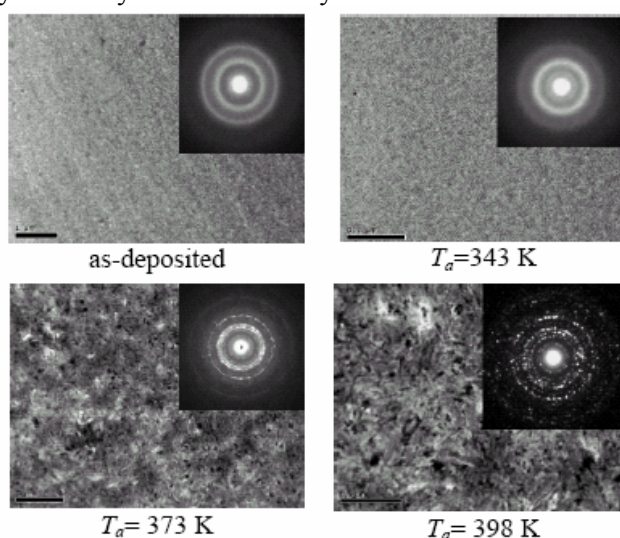


Fig.2 TEM micrograph and the corresponding electron diffraction pattern of the annealed AgSbSe₂ film. Film thickness 70 nm.

Fig.3 shows the EDX spectra for a typical representative sample of AgSbSe₂ films deposited onto glass substrate. The result indicates that the chemical composition of AgSbSe₂ films had elemental composition of 24.08:23.86:52.05 corresponding to Ag: Sb: Se, which indicating a deficiency in Ag (~0.92at %) and Sb (~1.14at %) with an excess of Se (~2.05at %) hence, led to consider that the as-deposited film had a chemical formula Ag_{0.963}Sb_{0.954}Se_{2.082}, revealing a nearly stoichiometric composition. A comparison between the elemental chemical compositions of the prepared bulk material, as-deposited films, and the calculated values are shown in the inset of Fig.3.

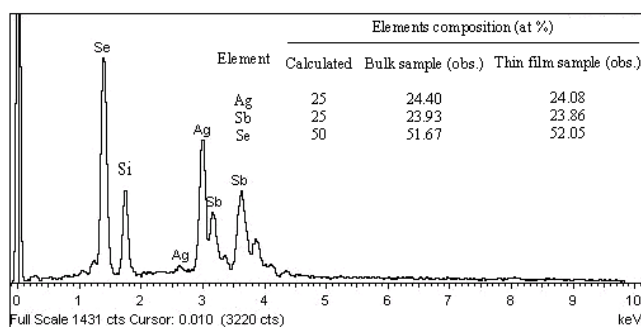


Fig. 3 EDX spectra of AgSbSe₂ film deposited onto glass substrate. Film thickness 780 nm.

3.2 Optical properties of AgSbSe₂ films

Fig.4 shows the transmission spectra of as-deposited AgSbSe₂ film of thickness 780 nm and another samples of the same film thickness annealed in Ar atmosphere for 1h, at annealing temperatures 343, 373 and 398 K. It was found that the absorption edge shifts towards lower energies as the annealing temperatures increases. Furthermore, the transmission was found to decrease with the increasing in the annealing temperatures.

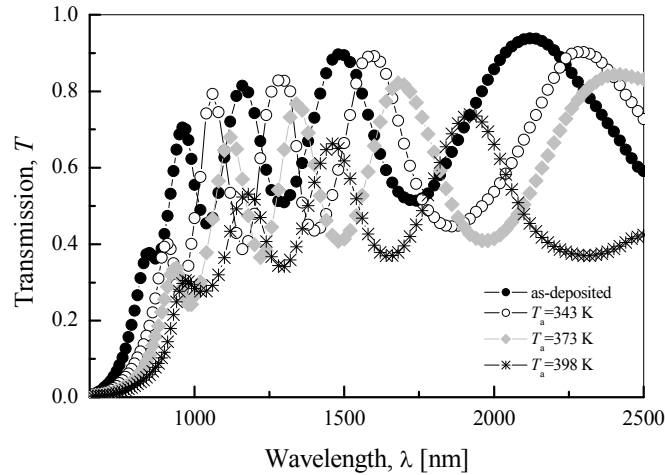


Fig. 4 Transmission spectra of AgSbSe₂ thin films annealed at different temperatures

The refractive index, n , film thickness and the order of interference of the investigated films were computed from the transmission spectra using the well-known Swanepole method [10] with $s=1.51$ (substrate refractive index). The sets of values of refractive index calculated according to the above mentioned method can be fitted to a reasonable function such as the two-term Cauchy dispersion relationship; $n(\lambda) = a + b/\lambda^2$; (where a and b are the Cauchy parameters) which can be used for extrapolation the refractive index to shorter wavelengths. The refractive indexes, n of AgSbSe₂ films annealed at different temperatures are shown in Fig.5.

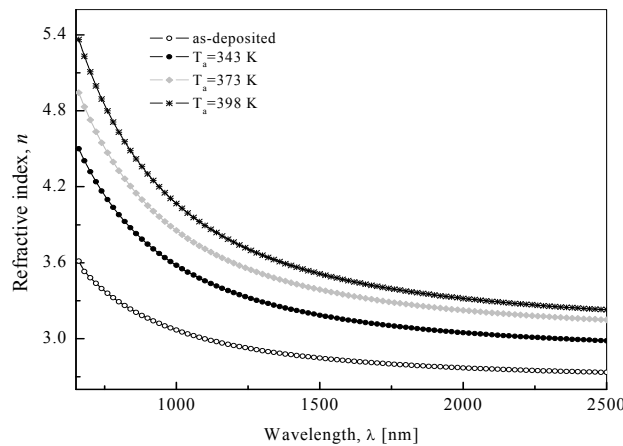


Fig.5 spectral distribution of refractive index, n for as-deposited and annealed AgSbSe₂ films.

As could be seen from the figure, the refractive index decreases with increasing wavelength and increases on increasing the annealing temperature. Wemple and DiDomenico [11]

have developed a model where the refractive index dispersion is studied in the region of transparency below the gap, using the single-effective oscillator approximation. Defining two parameters, the oscillator energy, E_o and the dispersion energy E_d this model concludes that:

$$n^2 = 1 + \frac{E_o E_d}{E_o^2 - E^2}, \quad (1)$$

Both Wemple parameters can be obtained from the slope and intercept of the plot $(n^2 - 1)^{-1} = f(E^2)$ with the y-axis as shown in Fig.6.

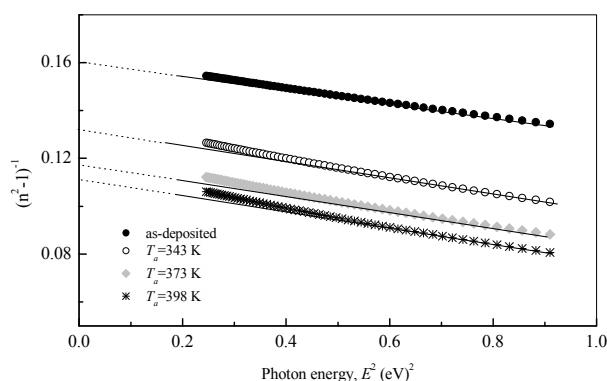


Fig. 6 plot of $(n^2-1)^{-1}$ vs. photon energy.

The values of Wemple-DiDomenico dispersion parameters, E_o , E_d static refractive index, n_o (calculated extrapolating the Wemple-DiDomenico optical-dispersion equation to, $E \rightarrow \infty$; ($n_o = 1 + E_d/E_o$)) as well as static dielectric constant, ϵ_s for the AgSbSe₂ films annealed at different temperatures are listed in Table 1. The oscillator energy E_o is related by an empirical formula to the optical gap value: $E_o \approx 2E_g$ [11]. The calculated values of the optical band gap are also presented in Table 1.

Table 1 Refractive index dispersion parameters.

T_a (K)	E_d (eV)	E_o (eV)	n_o	ϵ_s	$E_o/2 \approx E_g$ (eV)	$E_g^{ind.}$ (eV)
303	13.673	2.204	2.684	7.202	1.102	1.160
343	13.923	1.885	2.896	8.386	0.943	1.081
373	14.632	1.766	3.047	9.285	0.882	0.966
398	14.907	1.716	3.112	9.687	0.851	0.930

The obtained refractive index data can be further analyzed to obtain the high frequency dielectric constant via a procedure that describes the contribution of the free carriers and lattice vibration modes of the dispersion. The optical dielectric constant of AgSbSe₂ films was calculated using the relation [12].

$$\epsilon^{\bullet} = \epsilon_1 + i\epsilon_2 = (\epsilon_1^2 + \epsilon_2^2)^{1/2} \quad (2)$$

where ϵ_1 and ϵ_2 are the real and imaginary parts of the dielectric constant. The values of ϵ_1 and ϵ_2 for different incident photon energies can be obtained from the values of n and k ($k = \alpha\lambda/4\pi$) using the well-known relations:

$$\varepsilon_1 = n^2 - k^2, \quad \varepsilon_2 = 2nk \quad (3)$$

Since the reflectivity of a semiconductor in the NIR region shows anomalous dispersion as the incident photon energy approaches the corresponding value of plasma wavelength, λ_p . When $n^2 \gg k^2$ and $\omega\tau \ll 1$. The real dielectric constant can be expressed as [13]:

$$\varepsilon_1 = \varepsilon_L - [(\varepsilon_L \omega_p^2 / \omega^2)] ; \omega_p^2 = \frac{e^2 \cdot N/m^{\bullet}}{\varepsilon_o} \quad (4)$$

where ε_L is the lattice dielectric constant (or limiting value of the high frequency dielectric constant), ω_p the plasma frequency and ω is the angular frequency ($=2\pi c/\lambda$, c is the speed of light) of the lattice atoms, e is the electronic charge, N/m^{\bullet} carrier concentration to the effective mass ratio, and ε_o is the dielectric permittivity $8.85 \times 10^{-12} \text{ F/m}$. Therefore, plotting ε_1 vs. ω^2 in the NIR spectral region (not shown) allow us to determine the values of the plasma frequency, ω_p and lattice dielectric constant, ε_L from the slope and intercept, respectively. These calculated values are listed in Table 2. The observed disagreement between the values of static dielectric constant obtained according to Wemple and DiDomenico single-effective oscillator model and lattice dielectric constant obtained according to Eq.3 may be attributed to the contribution of the free carriers to the refractive index [14].

Table 2. values of ε_L , n , ω_p and N/m^{\bullet}

T_a [K]	ε_L	$n = \sqrt{\varepsilon_L}$	ω_p [$\times 10^{-15} \text{ s}^{-1}$]	N/m^{\bullet} [$\times 10^{22} \cdot \text{cm}^{-3}$]
303	7.983	2.825	4.39	1.04
373	9.694	3.157	7.51	1.48
398	11.009	3.318	9.19	1.66
423	11.464	3.386	9.46	1.73

The analysis of the absorption coefficient, α at the fundamnet absorption edge was found to follow the relation;

$$(\alpha \hbar \nu) = A \times (\hbar \nu - E_g)^p \quad (5)$$

where A is constant and the exponent p characterize the type of the optical transition. A plot of $(\alpha \hbar \nu)^{1/2}$ for as-deposited film and for those annealed at 343 and 378 K (shown in Fig.8-a) indicates a non direct optical transition with energy values 1.16, 1.08 and 0.97 eV, respectively. However, the analysis of the absorption coefficient for the film annealed at 398 K (Fig.8-b) indicated the presence of both direct and indirect optical transition with values of 0.96 and 0.93 eV, respectively.

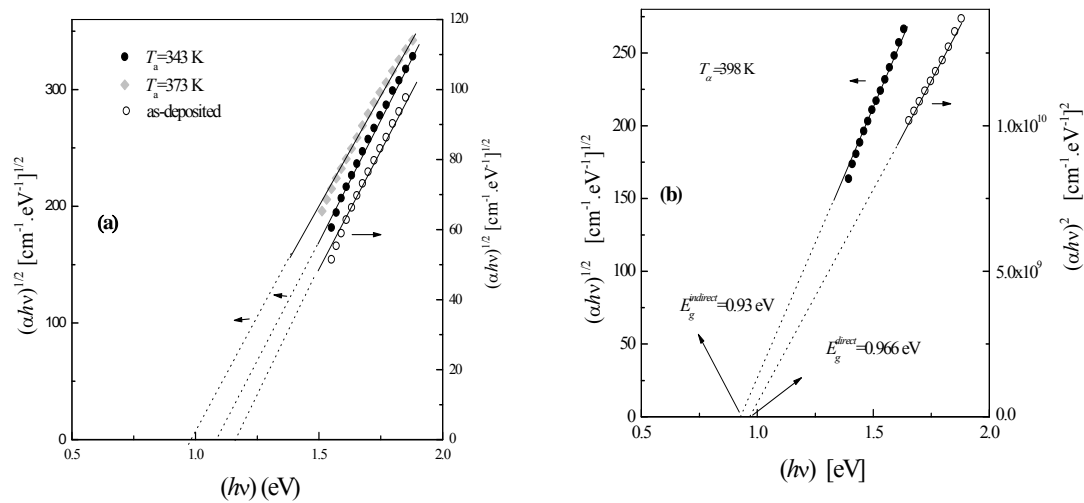


Fig. 7 a, b (a) plot of $(\alpha h\nu)^{1/2}$ for the as-deposited film and those annealed at 343 and 373 K vs. photon energy; and (b) plot of $(\alpha h\nu)^2$ and $(\alpha h\nu)^{1/2}$ for the film annealed at 398 K vs photon energy.

4. Conclusions

Nearly stoichiometric AgSbSe₂ thin films were deposited at room temperature by thermal evaporation onto glass substrates. The X-ray and electron diffraction studied revealed that the as-deposited films and those annealed at temperatures < 373 are amorphous in nature, while an amorphous-to-crystalline phase transition could be obtained for the films annealed at temperatures ≥ 373 K. Onset of main peaks corresponding to Ag₂Se and Sb₂Se₃ binary phases, beside the ternary AgSbSe₂ as a major phase were obtained when the film being annealed at 398 K. The effect of annealing temperature on the refractive index, high frequency dielectric constant (ϵ_∞), and carrier concentration to the effective mass ratio (N/m^*) were presented. The refractive index and consequently the high frequency dielectric constant were found to increase with the increase in the annealing temperatures. The analysis of the optical absorption coefficient for the deposited films revealed the presence of a non direct optical transition for as-deposited and those annealed at 343 and 373 K, while a direct and non direct optical transition for the film annealed at 398 K.

References

- [1] Pandey, N. Mehta, S. K. Tripathi, A. Kumar, Chalcogenide Letters **2**, 39 (2005).
- [2] M. A. Afifi, E. Abd El-Wahabb, A. E. Bekheet H. E. Atyia, J. Mat. Sci **41**, 7969 (2006).
- [3] M. Luo, M. Wuttig: Adv. Materials **16**, 439 (2004).
- [4] R. Detemple, D. Wamwangi, G. Bihlmayer, M. Wuttig, Appl. Phys. Lett. **83**, 2572 (2003).
- [5] J. Gutwirth, T. Wagner, P. Nemeč, S.O. Kasap, M. Frumar, Journal of Non-Crystalline Solids **354**, 497 (2008).
- [6] J. Li, L. Hou, H. Ruan, Q. Xie, F. Gan, Proc. SPIE **4085**, 125 (2001).
- [7] K. wang, C. Steimer R. Detemple, D. wamwangi. M wuttig, Appl. Phys. A **81**, 1601 (2005).
- [8] H. El-Zahed, Thin Solid Films **238**, 104 (1994).
- [9] Soliman, D Abdel-Hadyz and E Ibrahimz; J. Phys.: Condens. Matter **10**, 847 (1998).
- [10] R. Swanepoel, J. Phys. E **16**, 1214 (1983).
- [11] S.H. Wemple, M. Di Domenico, Phys. Rev. B **3**, 2767 (1971).
- [12] N. R. Koteeswara, K. T. R Ramakrishna, Material Research Bulletin **41**, 414 (2006).
- [13] A. Osama, M. M. Abdel-Aziz, I. S. Yahia, Applied Surface Science **255**, 4829 (2006).
- [14] M. Parlak, A. F. Qasrawi and C. Ercelebi; J. Mater. Sci. **38**, 1507 (2003).